in the middle of Figure 5 where the first four PE bands of **10** and **11** are correlated. Our correlation is based on ab initio calculations on **10** and **11** using a STO-3G basis adopting the geometrical parameters obtained from a X-ray study on **10** and **11**.[16] The wave functions that correspond to the four highest occupied MO's of **10** and **11** are shown schematically. The similarity with the four highest occupied MO's of **1** is evident. The correlation shown in the center of Figure 5 follows also from the nodal properties of the wave functions. In $8a_u$ and $7b_g$ there is a node through the heteroatoms, while in $11a_g$ and $10b_u$ large coefficients at the heteroatoms are predicted. Thus, in the latter case the difference in electronegativity between S and O is mainly responsible for the strong stabilization of $11a_g$ and $10b_u$ in the case of **11** as compared to **10**.

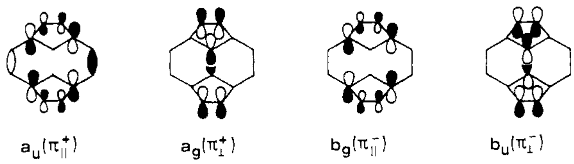

The comparison of the orbital sequence of **1** with that in **6a** led us to anticipate two effects for the comparison of **7a** with **10** and of **8a** with **11**: (i) a strong destabilization of $8a_u$ due to the increased σ/π interaction when a C_2H_4 bridge is replaced by a $Si_2(CH_3)_4$ bridge and (ii) a smaller split between $10b_u$ and $11a_g$ in the case of the sila-bridged species (**7a**, **8a**) as compared to **10** or **11**, respectively, caused by the larger separation of the π systems in **7a** and **8a**. Figure 5 shows the correlation between the PE bands of **7a** and **8a** and those of **10** and **11** using the criteria outlined above. As in the case of **6a**, one encounters in the PE spectra of **7a** and **8a** a high-lying σ band, which we ascribe tentatively to the ionization from the symmetric linear combination of the two Si-Si σ bonds (a_g). The assignment given in Figure 5 for **7a** and **8a** is also confirmed by MO calculations using the restricted HF theory employing a STO-3G basis[14] (see Table II). For these calculations we adopted for **7a** and **8a** the anti conformation of both heterorings and the same geometrical parameters of the thiophene and furan moiety as present in **10** and **11**.[16] For the Si-Si bond length we choose a value of 2.24 Å.

Conclusions

Our PE investigations on **6a**-**8a** reveal in all three cases a very strong interaction between the π MO of b_{3u} (**6a**) and $8a_u$ (**7a**, **8a**) symmetry, respectively, and the corresponding MO's mainly localized at the Si-Si σ bonds. The comparison between **1**, **3**, and **6a** (Figure 3) shows that the σ/π interaction of a highly strained C-C σ bond, as present in the cyclopropane moieties of **3**, is comparable to the Si-Si σ bond of **6a**. The comparison of the first PE bands of **7a**-**10** and **8a**-**11** indicates the same sequence of the highest occupied MO's in all four compounds; the comparison **1**-**6a**, however, yields a reversal of the HOMO. This finding is of interest with respect to the ESR spectra of the corresponding radical cations and reactions in which the symmetry of the HOMO is a determining factor.

Experimental Section

The syntheses of **6a**-**8a** have been reported in the literature.[7,8] The He I photoelectron spectra of the analytically pure compounds were recorded on a Perkin-Elmer PS 18 spectrometer. The recording temperatures were as follows: **6a** and **7a**, 140 °C; **8a**, 90 °C. The spectra were calibrated with argon and xenon. An estimated accuracy of ±0.05 eV was achieved for the single bands and of ±0.1 eV for the shoulders.

Acknowledgment. Financial support is gratefully acknowledged by the Fonds der Chemischen Industrie and the BASF Aktiengesellschaft in Ludwigshafen. We thank A. Flatow for measuring the PE spectra.

Registry No. 6a, 109828-61-7; **6b**, 114184-43-9; **7a**, 114184-41-7; **7b**, 114197-84-1; **8a**, 114184-42-8; **8b**, 114184-44-0.

---

[16] Bresciani-Pahor, N.; Calligaris, M.; Rondaccio, L. *J. Chem. Soc., Perkin Trans. 2* **1978**, 42.

High Molecular Weight Boron Oxides in the Gas Phase

Robert J. Doyle, Jr.

Contribution from the Chemistry Division, Code 6112, Naval Research Laboratory, Washington, D.C. 20375-5000. *Received December 9, 1987*

Abstract: A new class of gas-phase boron oxides has been produced by particle-induced desorption from vitreous boron trioxide. Six distinct homologous series of boron oxide cations were identified by fast atom bombardment mass spectrometry and studied by collision-induced dissociation. Common structural features within each series were confirmed by the identification of common collision-induced fragments. Two important series are described by the general formulas $[B_{2n+1}O_{3n+1}]^+$ (n = 0–6) and $[B_{2n+2}O_{3n+3}]^{\bullet+}$ (n = 0–4). Ions of the first series show the highest relative abundances in the desorption spectrum of boron trioxide and are the most abundant ionic fragments in the collision spectra of nearly all boron oxide cations. The most important of these is $[B_3O_4]^+$, which is proposed to exist as $[O{=}B{-}O{-}B{-}O{-}B{=}O]^+$ and is stabilized by extensive resonance and electron sharing. Gas-phase boron oxide cations are proposed to exist with boron limited to two- or three-coordination with oxygen. The ions are thus built upon integral BO_3 triangles, and branches are terminated with $-B{=}O$ units.

Polymeric boron oxide anions, in the form of polyborate ions, are well-known components of crystalline borate salts.[1] Although simple boron–oxygen cations and anions such as BO^+, $B_2O_3^{\bullet+}$, and BO_2^- have been isolated in the gas phase, there has been no evidence for the existence of polymeric boron–oxygen species in the gas phase. The difficulty of predicting the existence of such species arises from structural uncertainties because of the interchangeability of boron coordination.

Boron–oxygen compounds are observed typically with boron assuming a three- or fourfold coordination with oxygen. The most common oxidation state of boron (+3) is the result of sp^2 hybridization that is responsible for the formation of three triangular-planar bonds with oxygen. The low-energy fourth orbital of the boron valence shell is responsible for its Lewis acid prop-

---

[1] Muetterties, E. L. *The Chemistry of Boron and Its Compounds*; Wiley: New York, 1967; pp 166–176.

[2] White, D.; Walsh, P. N.; Mann, D. E. *J. Chem. Phys.* **1958**, *28*, 508–509. White, D.; Mann, D. E.; Walsh, P. N.; Sommer, A. *J. Chem. Phys.* **1960**, *32*, 481–487.

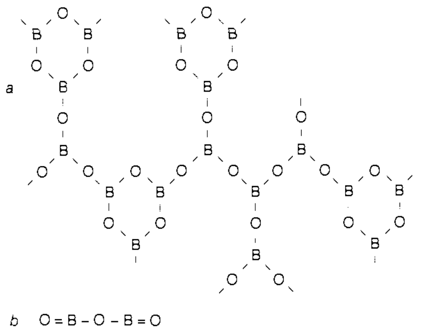

Figure 1. (a) One proposed structure of condensed-phase, vitreous boron trioxide; (b) gas-phase B_2O_3. True bond angles are not represented.

erties. The acceptance of an electron pair into this orbital results in sp^3 hybridization and fourfold tetrahedral coordination.

Twofold linear coordination of boron to oxygen by π-bonding to one oxygen atom was first proposed to exist in isolated B_2O_3[2] and HOBO[3] molecules. The infrared emission spectra of gas-phase B_2O_3 and HOBO revealed stretching frequencies that were accounted for in terms of $-B{=}O$ bonds.[2] The infrared absorption spectra of B_2O_3 in solid argon matrices also revealed stretching frequencies that were concluded to be the result of $-B{=}O$ bonds.[4,5] Electron diffraction experiments indicated twofold coordination of boron in gas-phase alkali metaborates.[6] The mass spectra of substituted boroxines showed fragment ions whose structures were rationalized with the proposal of $-B{=}O$ terminal units.[7] The decreasing association of liquid boron trioxide (B_2O_3) with increasing temperature was explained by the proposal of the transition of three-coordinated boron to two-coordinated boron with the attending formation of terminal $-B{=}O$ bonds.[8] This last proposal may be an important link between the condensed-phase structure of B_2O_3 and its gas-phase oligimers.

The structure of vitreous boron trioxide has been investigated by X-ray,[9] NMR,[10] and neutron diffraction[11] techniques. In all three cases, the results were interpreted to support the existence of a random network of boroxol rings. The most recent study emphasized that the boroxol rings were interconnected by a random number of BO_3 triangles[11] (Figure 1a). An X-ray diffraction study of molten boron trioxide (650 °C) concluded that the melt contained a mixture of boroxol rings linked by independent BO_3 units.[12] Dissenting opinions, based on computer modeling[13] and molecular dynamics calculations,[14] hold that the structure of vitreous boron trioxide can be understood on the basis of a continuous random network of BO_3 triangles containing no boroxol rings at all. Clearly, the long-debated question of the structure of vitreous B_2O_3 has not been resolved satisfactorily.

In spite of the disagreement between the experimentally derived and the theoretically derived structures of vitreous B_2O_3, a foundation for the structures of gas-phase cationic species generated from B_2O_3 can be constructed from structural features that are common to both. For example, the absence of boron–boron bonds in condensed-phase B_2O_3 suggests that gas-phase polymers will also lack boron–boron bonds (assuming the absence of ion-molecule reactions). Furthermore, the three-coordination of boron with oxygen in condensed-phase B_2O_3 suggests that BO_3 units are likely to be integral parts of gas-phase polymers. Finally, the early proposal that terminal $-B{=}O$ units are formed in the high-temperature melt of B_2O_3[8] in addition to the proposed structure of gas-phase B_2O_3[2,4,5] (Figure 1b) suggests that $-B{=}O$ units may be terminal structural elements essential to the stability of polymeric gas-phase ions and neutrals.

Investigations into the behavior of gas-phase B_2O_3 have been limited because of the extremely low vapor pressure of condensed-phase boron trioxide.[15] Boron oxide vapors, produced in an effusion cell at temperatures in excess of 1000 °C, have been examined mass spectrometrically.[5,15] The cationic species B^+, BO^+, $B_2O_2^{\bullet+}$, and $B_2O_3^{\bullet+}$, were identified. Secondary ion mass spectrometry (SIMS) showed that B^+, BO^+, BO^-, and BO_2^- ions were produced by the bombardment of the surface of crystalline B_2O_3 with inert-gas ions.[16]

Another well-known particle-bombardment technique, fast atom bombardment (FAB),[17] has been applied to the analysis of the surfaces of insulating materials such as multicomponent glasses for the purpose of quantitative elemental analysis.[18] The high-energy beam of inert-gas atoms produces a significant yield of sputtered sample ions while problems associated with sample charging are eliminated. It is with this technique that high-order boron oxide ions have been generated from vitreous boron trioxide and studied by mass spectrometry.

Experimental Section

Samples of crystalline B_2O_3 (mp 450 °C) were heated in air at 1000 °C for a minimum of 4 h. The crystalline form of B_2O_3 converts to the vitreous (glass) form at 450 °C and does not revert to the crystalline form upon cooling at ambient pressure.[19] The flat surface of an FAB sample holder was dipped into the melt and scraped to produce a relatively thin film. The sample holder was then attached to the FAB probe and inserted into the FAB ion source of a ZAB-2F (V. G. Analytical, Ltd.) mass spectrometer. The ZAB-2F is a double-focusing, reverse-geometry instrument; the magnetic sector precedes the electric sector. The FAB sample holder is a new design capable of heating the sample to 650 °C.[20] The B_2O_3 sample was then heated in vacuo (10^{-8} Torr, gauge reading) at 600 °C for a minimum of 1 h. The sample temperature was then adjusted to between 100 and 600 °C during the acquisition of mass spectra. Continuous heating of the sample is necessitated by the extreme hygroscopicity of B_2O_3.[20,21]

The FAB saddle-field gun (Ion Tech, Ltd.) was operated at 8 kV with a current of 1.8 mA. The xenon gas supply to the gun increased the background source pressure to 10^{-6} Torr (gauge reading). The mass spectrometer was operated with an accelerating voltage of 8 kV. All slits were fully open for maximum sensitivity.

Mass spectra were obtained by signal addition; a minimum of 64 scans was acquired at each temperature. The atomic compositions of boron oxide ions were determined by isotope ratios based on $^{11}B/^{10}B$ equal to 4.00. The heights of isotopic peaks were summed to yield the absolute abundance of each ion.

Mass spectra were taken at B_2O_3 sample temperatures varied from 100 to 600 °C in 100 °C steps. There were no observed variations in total ion abundances or relative ion abundances over this temperature range. This is not surprising in light of the considerable amount of energy imparted to the sample by the incident Xe beam. The translational energy of the majority of Xe atoms generated with an 8-kV FAB gun anode potential has been estimated to lie between 6.5 and 6.7 keV.[22] One recent study of the charge stripping of metal ions generated by the FAB of various salt samples concluded that a primary argon atom beam with an 8-kV anode potential is capable of transferring up to approximately 30 eV of internal energy during the ionization process.[23] Accordingly, the internal energy of product ions is largely controlled by the

---

(3) White, D.; Mann, D. E.; Walsh, P. N.; Sommer, A. *J. Chem. Phys.* **1960**, *32*, 488–492.

(4) Weltner, W., Jr.; Warn, J. R. W. *J. Chem. Phys.* **1962**, *37*, 292–303.

(5) Sommer, A.; White, D.; Linevsky, M. J.; Mann, D. E. *J. Chem. Phys.* **1963**, *38*, 87–98.

(6) Ezhov, Y. S.; Tolmachev, S. M. *Zh. Strukt. Khim.* **1972**, *13*, 972–976.

(7) Brooks, C. J. W.; Harvey, D. J.; Middleditch, B. S. *Org. Mass Spectrom.* **1970**, *3*, 231–235.

(8) Mackenzie, J. D. *J. Phys. Chem.* **1959**, *63*, 1875–1878.

(9) Mozzi, R. L.; Warren, B. E. *J. Appl. Crystallogr.* **1970**, *3*, 251–257.

(10) Jellison, G. E.; Panek, L. W.; Bray, P. J.; Rouse, G. B., Jr. *J. Chem. Phys.* **1977**, *66*, 802–812.

(11) Sinclair, R. N.; Desa, J. A. E.; Etherington, G.; Johnson, P. A. V.; Wright, A. C. *J. Non-Cryst. Solids* **1980**, *42*, 107–116.

(12) Miyake, M.; Suzuki, L.; Morikawa, H.; Takagi, Y.; Marumo, F. *J. Chem. Soc., Faraday Trans. 1* **1984**, *80*, 1925–1931.

(13) Elliott, S. R. *Philos. Mag. B* **1978**, *37*, 435–446.

(14) Soules, T. F. *J. Chem. Phys.* **1980**, *73*, 4032–4036.

(15) Nikitin, O. T.; Akishin, P. A. *Dokl. Akad. Nauk. SSSR* **1962**, *145*, 1294–1296.

(16) Joyner, D. J.; Hercules, D. M. *J. Chem. Phys.* **1980**, *72*, 1095–1108.

(17) Barber, M.; Bordoli, R. S.; Elliot, G. J.; Sedgewick, R. D.; Tyler, A. N. *Anal. Chem.* **1982**, *54*, 645A–657A.

(18) Surman, D. J.; Vickerman, J. C. *Appl. Surf. Sci.* **1981**, *9*, 108–121.

(19) Gurr, G. E.; Montgomery, P. W.; Knutson, C. D.; Gorres, B. T. *Acta Crystallogr., Sect. B: Struct. Crystallogr. Cryst. Chem.* **1970**, *B26*, 906–915.

(20) Doyle, R. J., Jr. *Anal. Chem.* **1987**, *59*, 537–539.

(21) Shmidt, N. E. *Russ. J. Inorg. Chem.* **1966**, *11*, 241–247.

(22) Alexander, A. J.; Hogg, A. M. *Int. J. Mass Spectrom. Ion Processes* **1986**, *69*, 297–311.

(23) Rabrenovic, M.; Ast, T.; Beynon, J. H. *Int. J. Mass Spectrom. Ion Processes* **1984**, *61*, 31–40.

Table I. Six Homologous Series of Boron Oxide Cations

formula index (n)	series number: general formula					
	I: $[B_{2n+1}O_{3n}]^+$	II: $[B_{2n+1}O_{3n+1}]^+$	III: $[B_{2n+2}O_{3n+1}]^{\bullet+}$	IV: $[B_{2n+1}O_{3n+2}]^+$	V: $[B_{2n+2}O_{3n+2}]^{\bullet+}$	VI: $[B_{2n+2}O_{3n+3}]^{\bullet+}$
0	B^+	$[BO]^+$	$[B_2O]^{\bullet+}$	$[BO_2]^+$	$[B_2O_2]^{\bullet+}$	$[B_2O_3]^{\bullet+}$
1	$[B_3O_3]^+$	$[B_3O_4]^+$	$[B_4O_4]^{\bullet+}$	$[B_3O_5]^+$	$[B_4O_5]^{\bullet+}$	$[B_4O_6]^{\bullet+}$
2	$[B_5O_6]^+$	$[B_5O_7]^+$	$[B_6O_7]^{\bullet+}$	$[B_5O_8]^+$	$[B_6O_8]^{\bullet+}$	$[B_6O_9]^{\bullet+}$
3	$[B_7O_9]^+$	$[B_7O_{10}]^+$	*a*	$[B_7O_{11}]^+$	$[B_8O_{11}]^{\bullet+}$	$[B_8O_{12}]^{\bullet+}$
4	$[B_9O_{12}]^+$	$[B_9O_{13}]^+$				$[B_{10}O_{15}]^{\bullet+ b}$
5		$[B_{11}O_{16}]^{+ b}$				
6		$[B_{13}O_{19}]^{+ b}$				

[a] $[B_8O_{10}]^+$ was not observed. [b] Not shown in Figures 2 or 3.

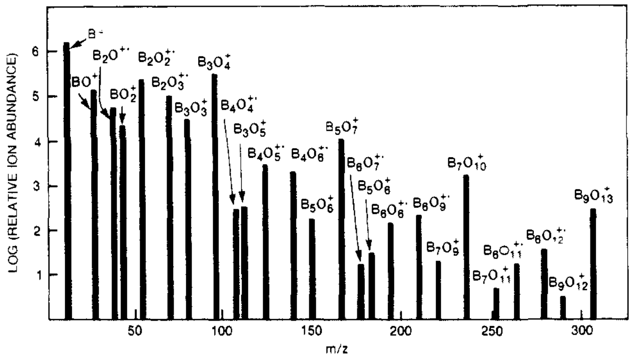

Figure 2. Fast atom bombardment mass spectrum of molten boron trioxide. Peak heights represent the sum of all isotopic contributions. The melt temperature was 550 °C.

energy of the incident primary beam and should be nearly independent of sample temperature over the temperature range used in these experiments.

Collisional activation (CA) mass spectra[24] were obtained by mass selection of each $^{11}B_xO_y$ isotope by the magnetic sector, interaction with helium gas in a collision cell located between the magnetic and electric sectors, and subsequent energy/mass analysis by the electric sector. The helium pressure in the second field-free region collision cell was 10^{-6} Torr (gauge reading). The main beam was thereby decreased by approximately 50%, a condition that corresponds to multiple collisions. Spectra were obtained by signal addition, and fragment ion abundances were determined by peak-height ratios.

Results and Discussion

The fast atom bombardment of vitreous boron trioxide produces a large number of singly charged boron oxide cations. Figure 2 shows the relative abundances (logarithmic) of all boron-containing ions below m/z 310 in the FABMS of B_2O_3. Also observed were $[B_{10}O_{15}]^{\bullet+}$, $[B_{11}O_{16}]^+$, and $[B_{13}O_{19}]^+$ whose low abundances could not be measured accurately. All of the boron oxide cations with more than two boron atoms are reported here for the first time.

The prominent feature of Figure 2 is the local abundance maxima exhibited by four ions. It will be shown that the relationship between these ions is also shared by five other groups of boron oxide ions. Ultimately, this relationship leads to the codification of all boron oxide ions into six homologous series with common structural features within each series. First, local abundance maxima are exhibited by $[B_3O_4]^+$, $[B_5O_7]^+$, $[B_7O_{10}]^+$, and $[B_9O_{13}]^+$. These ions are related by a difference of two boron atoms and three oxygen atoms (B_2O_3) between each subsequent ion. For example, the addition of one, two, and three B_2O_3 units to $[B_3O_4]^+$ will form each of the other three ions in this series (disregarding structure). The series may be described by the general formula $[B_{2n+1}O_{3n+1}]^+$ where $n = 1$–4. If $n = 0$, $[BO]^+$ is included as the first element of the series.

Likewise, the quasi-molecular ion,[25] $[B_2O_3]^{\bullet+}$, and its multimers, $[B_4O_6]^{\bullet+}$, $[B_6O_9]^{\bullet+}$, and $[B_8O_{12}]^{\bullet+}$, are related by additions of B_2O_3 and may be described by the general formula $[B_{2n+2}O_{3n+3}]^{\bullet+}$, where $n = 0$–3. In fact, every ion in the boron oxide ion distribution may be classified as a member of one of six series in which the members are related by additions (or subtractions) of B_2O_3 units. The scheme is presented in tabular form in Table I.

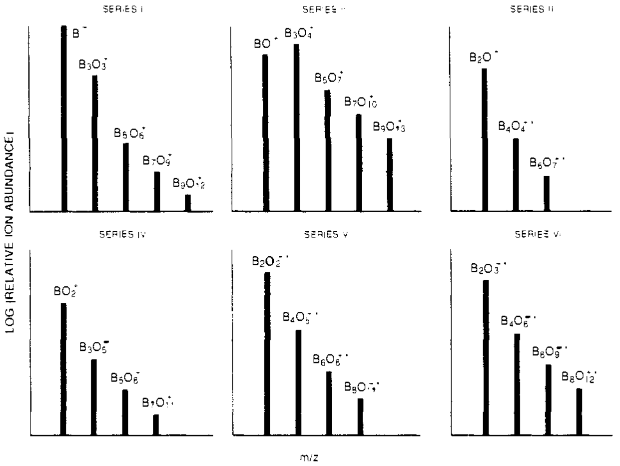

Figure 3. Relative ion abundances of the six series of boron oxide ions. Ions within each series are related by differences of B_2O_3 units.

The rows of Table I list ions in the order of their mass to charge ratios (m/z). The columns thus formed contain the elements of each series that are related by additions of B_2O_3. When one reads down each column, it can be seen that each series element can be formed by the addition of B_2O_3 to the preceding element. A general formula for the elements of each series is presented at the top of each column.

Figure 3 presents graphically the deconvolution of the six series from Figure 2. The ions within each series exhibit monotonically decreasing abundances with increasing m/z. $[B_3O_4]^+$ (series II) is anomalous in this respect, and its high abundance may be due to its unusual stability. Note also that each series is composed of ions containing only an even number or only an odd number of boron atoms, and therefore each series contains only odd or only even electron ions. Although the intraseries relationships discussed so far present some basis for suspecting unique structural features for each series, evidence for this is tenuous at best without a direct structural probe. As will be shown below, structural information provided by collisional activation provides a solid unifying factor between members of each series in the form of the marked similarity between their collisionally activated mass spectra.

Collisional activation (CA) mass spectra can often provide structural information and information concerning ion behavior. The majority of high-energy CA reactions involve simple bond cleavages, and therefore the relative abundances of CA product ions can be directly related to the parent-ion structure.[26] There are, however, limitations to the utility of CA mass spectra in structure determination. Collision-induced fragmentation cannot, by itself, adequately differentiate between structural isomers. The assignment of isomeric ion structures requires far more involved

---

(24) Cooks, R. G.; Beynon, J. H.; Caprioli, R. M.; Lester, G. R. *Metastable Ions*; Elsevier: New York, 1973.

(25) B_2O_3 is the empirical formula of condensed-phase boron trioxide. The term *molecule* has no meaning for a vitreous material, and therefore the use of the term *molecular ion* would be incorrect. *Quasi-molecular ion* is used here to represent the gas-phase ion whose formula corresponds to the empirical formula of condensed-phase boron trioxide.

(26) Cooks, R. G. In *Collision Spectroscopy*; Cooks, R. G., Ed.; Plenum: New York, 1978; pp 357–450.

Table II. CA Mass Spectra of Boron Oxide Cations Derived from FAB of B_2O_3

		neutral loss (relative abundance)												
series	ion	$^{\bullet}B$	O	$^{\bullet}BO$	$^{\bullet}BO_2$	B_2O_2	B_2O_3	$^{\bullet}B_3O_3$	B_2O_4	$^{\bullet}B_3O_4$	$^{\bullet}B_3O_5$	B_4O_6	$^{\bullet}B_5O_8$	B_6O_9
I	$B_3O_3^+$			100	7	13								
	$B_5O_6^+$					100								
II	$B_3O_4^{+b}$			100	73	8	7							
	$B_5O_7^+$						100			8	6			
	$B_7O_{10}^+$						100					57		
	$B_9O_{13}^+$						100					10		6
III	$B_2O^{\bullet+}$	100	5	64										
	$B_4O_4^{\bullet+}$			64		100								
	$B_6O_7^{\bullet+a}$			100		100		39						
IV	$B_3O_5^{+b}$		100	7	69									
V	$B_2O_2^{\bullet+}$	21	15	100	10									
	$B_4O_5^{\bullet+}$				100	8	10							
	$B_6O_8^{\bullet+}$			100			9			35				
VI	$B_2O_3^{\bullet+}$		100	41	27									
	$B_4O_6^{\bullet+}$				100		23		9					
	$B_6O_9^{\bullet+}$			23	100		55				58	7		
	$B_8O_{12}^{\bullet+}$				100		45				9		10	

[a] $S/N = 4$. For all other spectra $S/N > 10$. [b] $[BO]^+$ (series II) and $[BO]^+$ (series IV) could not be resolved from interfering species.

methods including the determination and evaluation of thermochemical data.[27] Because this is the first report of the existence of gas-phase boron oxide ions (containing more than two boron atoms), no thermochemical data exist. Furthermore, the determination of ionization energies and appearance energies is not possible with the FAB technique. As a result of these limitations, CA spectra will be interpreted in terms of all reasonable isomers of each species. It is therefore one of the objects of this report to establish a qualitative picture of the bonding and coordination in gas-phase boron oxide ions.

Table II presents the numerical results of CA mass spectra for all boron oxide ions of sufficient abundance to generate reproducible spectra. Mass-selected parent ions are grouped according to the six series shown in Figure 3. In the discussion of possible structures of boron oxide ions derived from CA mass spectra, each series will be considered independently. Only three series, series II, V, and VI, will be examined in detail. Common features within each series will be emphasized, and where possible, explanations for unusual stability will be explored. In cases where numerous structural isomers are consistent with a CA mass spectrum, only those isomers that represent the general trends of isomerization within a series will be shown. The details of bond breaking in parent ions and bond formation in fragment ions are straightforward and will not be shown.

(1) CA Mass Spectra of Series II Ions. The relatively high abundance series II ions are used as structural archetypes for the other five series of boron oxide ions. As shown in Figure 2 and Table II, series II ions exhibit local abundance maxima in the FABMS of boron trioxide and appear as the most abundant dissociation products in most of the CA spectra of individual boron oxide ions. The most important factor influencing the abundance of a product ion is its stability.[28] Although this rule has exceptions (rearrangement reactions for which there is a significant reverse activation energy, for example[29]), the evidence for the unusual stability of series II ions is substantial in light of the aforementioned observations.

The foundation on which rests the structures of series II ions, and hence most other boron oxide ion structures, is the structure of $[B_3O_4]^+$. The proposed structure of $[B_3O_4]^+$ (**1**–**3**) is based upon two considerations. First, the accepted structure of the gas-phase B_2O_3 molecule (Figure 1b) establishes that twofold coordination of boron to oxygen, in the form of –B═O units, provides a stable termination of the isolated molecule in the gas phase. Second, the proposed structure of $[B_3O_4]^+$ incorporates two important types of ion stabilization: electron sharing and resonance stabilization.[28] Electron sharing between structures **1** and **2** and between structures **2** and **3** involves electrons from the nonbonding orbitals of the oxygen atoms. Electron sharing is enhanced by the tendency of nonbonding electrons from small atoms (fluorine, for example) to be partially back-donated to boron. This reduces the electron deficiency on boron and apparently outweighs the opposing inductive effect expected from the greater electronegativity of the small heteroatom.[30] Resonance stabilization of $[B_3O_4]^+$ can be seen in the two equivalent resonance forms, structures **1** and **3**. It is suggested that the two types of ion stabilization, working in concert, are particularly effective at charge delocalization and bond equilization. The consequential lower energy of the ion is thus responsible for its exceptional relative stability.

1 $O{=}B{-}O{-}B{=}\overset{+}{O}{-}B{=}O$

2 $O{=}B{-}O{-}\overset{+}{B}{-}O{-}B{=}O$

3 $O{=}B{-}\overset{+}{O}{=}B{-}O{-}B{=}O$

The CA spectrum of $[B_3O_4]^+$ is consistent with the proposed structure. Bond cleavage is seen to occur at every bond except the terminal B═O bond. Loss of $^{\bullet}BO$ to form $[B_2O_3]^{\bullet+}$ predominates.

All of the proposed structures for series II ions exhibit the stabilizing features found in $[B_3O_4]^+$. The remaining members of series II show facile loss of B_2O_3 to form another series II ion. All may exist as cyclic structures containing one boroxol ring or as acyclic structures. $[B_5O_7]^+$ is proposed to exist as structure **4**, containing a boroxol ring, or as the acyclic structure **5**. Both structures are consistent with the CA mass spectrum of $[B_5O_7]^+$. The preferred dissociation pathway is through the loss of B_2O_3. Structure **4** may lose B_2O_3 by a retro Diels–Alder (RDA) type cleavage at a and b. Structure **5** may lose B_2O_3 by cleavage at a. The ionic product resulting from the loss of B_2O_3 from either **4** or **5** is **2**. The less probable neutral losses may occur from either structure. It is not possible to distinguish between **4** and **5** by collision-induced dissociation. Indeed, structure **4** may convert directly to structure **5** by ring opening at b or c.

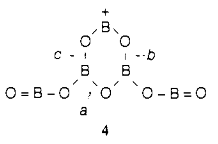

4

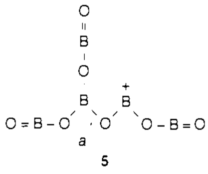

5

Four isomeric structures of $[B_7O_{10}]^+$ are shown as structures **6**–**9**. Structure **7** may assume the acyclic structure of **6** or **8** by

---

(27) Holmes, J. L. *Org. Mass Spectrom.* **1985**, *20*, 169–183.

(28) McLafferty, F. W. *Interpretation of Mass Spectra*; University Science: Mill Valley, CA, 1980; pp 46–47.

(29) Wagner, W.; Heimbach, H.; Levsen, K. *Int. J. Mass Spectrom. Ion Processes* **1980**, *36*, 125–142.

(30) Helsop, R. B.; Jones, K. *Inorganic Chemistry*; Elsevier: Amsterdam, The Netherlands, 1976; p 334.

ring opening at a or b. Structure **9** cannot assume a stable acyclic structure by ring opening. Three of the four isomers, **7**–**9**, can accommodate the favorable loss of B_2O_3, structure **7** by an RDA-type reaction with ring cleavage at b and c, structure **8** by bond breaking at a, and structure **9** by bond breaking at a. The ionic product formed by the loss of B_2O_3 from structures **7** and **8** is structure **5**. Loss of B_2O_3 from structure **9** yields structure **4**. Loss of B_2O_3 from structure **9** by an RDA-type reaction with ring cleavage at b and c will not yield a stable ionic product. Structure **6** cannot lose B_2O_3 by simple cleavage. The loss of B_4O_6 by collisional activation is possible for only structures **6** and **7**, from structure **6** by cleavage at a or b and from structure **7** by ring cleavage at a and d. In both cases the ionic product is **2**. The final ion in series II, $[B_9O_{13}]^+$, has at least five isomeric structures that are consistent with its CA mass spectrum and will not be considered in detail here.

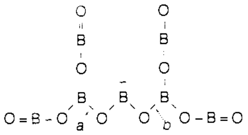
6

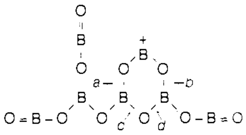
7

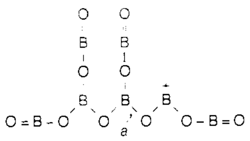
8

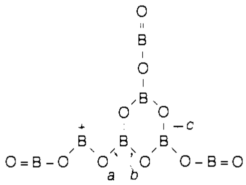
9

Of the acyclic structures of series II ions (cyclic structures are discussed separately below), those exhibiting symmetry around $O-B^+-O$ may experience a greater degree of stabilization. This is a consequence of the hybridization of the nearest-neighbor boron atoms. Similar to carbon,[31] the greater the s character in an sp^n-hybridized atomic orbital, the greater the electronegativity of the hybridized boron orbital. Accordingly, the boron atomic orbital of a $-B{=}O$ unit (sp hybrid) will be more electronegative than the boron atomic orbital of a BO_3 unit (sp^2 hybrid). As a result, asymmetric isomers such as structure **8** will demonstrate a preference for the resonance form with the $-^+O{=}B^-$ double bond directed toward the less electronegative BO_3 unit. Bond equalization cannot then be fully realized. Symmetric isomers such as structure **6** will show no preference for either resonance form, and bond equalization and the attendant lowering of energy will be realized.

It should be reemphasized that no attempt has been made to differentiate between structural isomers. Indeed, they cannot be distinguished on the basis of the data presented here. In addition, it should be noted that isomers containing boroxol rings, for example, structure **7**, may also represent easily accessible transition states in the dissociation of acyclic isomers (structures **6** and **8** in this example).

As mentioned in the introduction, there is some disagreement concerning the presence of boroxol rings in condensed-phase boron trioxide. Although their presence in gas-phase boron oxide ions cannot be confirmed by this study, the exceptional stability of other gas-phase species incorporating boroxol rings mandates consideration of boroxol-ring-containing boron oxide ions. The concept of aromaticity in boroxol rings has been debated for some time.[32] Although there is no firm consensus on the degree of stabilization conferred by delocalization of electrons in the boroxol ring, there is some agreement that they are indeed aromatic.[32] This is supported by NMR and mass spectrometry studies of methyl-substituted boroxine that indicated ring stabilization by cyclic π-conjugation of the 6π-electron system.[33,34] The unusual stability of the methyl-substituted borenium ion was explained when the same argument was invoked.[33] Accordingly, several proposed boron oxide ions are shown to incorporate a boroxol ring.

In summation, series II boron oxide ions exhibit enhanced stability over the other five boron oxide series. The enhanced stability can be accounted for in terms of resonance stabilization and electron sharing that can be represented by canonical forms analogous to structures **1**–**3**. Dissociation by collisional activation is dominated by loss of B_2O_3 or a multimer of B_2O_3 and yields a series II ion.

(2) CA Mass Spectra of Series V Ions. The CA mass spectrum of $[B_2O_2]^{\bullet+}$ implies that it is not the cationic analogue of the isolated B_2O_2 molecule. The B_2O_2 molecule has been shown to be linear with a central B–B bond[2] (**10**). However, the CA mass spectrum of $[B_2O_2]^{\bullet+}$ shows the loss of $^\bullet B$ and the loss of $^\bullet BO_2$, which can occur only from an ion of structure **11**. Nevertheless, it should be emphasized that a $[B_2O_2]^{\bullet+}$ ion with a structure analogous to **10** would also likely dissociate by losses of $^\bullet BO$ and O, which are observed. Although structure **11** is consistent with the structure of condensed-phase boron trioxide, the high internal energy of the desorbed ion may promote pre- or postcollisional rearrangement prior to dissociation. Accordingly, it cannot be demonstrated that one or the other ion is desorbed from condensed-phase boron trioxide; it can only be demonstrated that the previously unobserved $[B_2O_2]^{\bullet+}$ isomer (**11**) is present prior to dissociation.

$O=B-B=O$
10

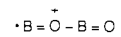
$\cdot B=\overset{+}{O}-B=O$
11

An acyclic, nonbranching structure may be proposed for $[B_4O_5]^{\bullet+}$. Three resonance forms of this structure are shown (**12**–**14**); three additional resonance forms are equivalent to 180° rotation about the central oxygen atom of each form shown.

12
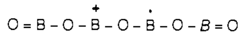
$O=B-O-\overset{+}{B}-O-\overset{\cdot}{B}-O-B=O$

13
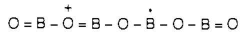
$O=B-\overset{+}{O}=B-O-\overset{\cdot}{B}-O-B=O$

14
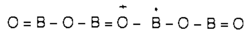
$O=B-O-B=\overset{+}{O}-\overset{\cdot}{B}-O-B=O$

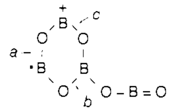
15

Structure **15** is the proposed cyclic form. The loss of $^\bullet BO$ is the dominant CA process, and the proposed acyclic form of $[B_4O_5]^{\bullet+}$ can lose $^\bullet BO$ by simple cleavage with coincident formation of $[B_3O_4]^+$ (**2**). The losses of B_2O_2 and B_2O_3 may likewise occur from the acyclic structure by simple bond cleavage. The cyclic form (**15**) may lose $^\bullet BO$ by ring cleavage at a and b. B_2O_2 and B_2O_3 may be lost by ring cleavage at b and c, the neutral loss depending on which fragment retains the charge.

Structures **16**–**18** are proposed for $[B_6O_8]^{\bullet+}$. The formation of a series II ionic product ($[B_5O_7]^+$) is the driving force behind the loss of $^\bullet BO$ from each of the three proposed structures, structures **16** and **17** forming the branched isomer (**5**) and structure **18** forming the cyclic isomer (**4**). The significant loss of $^\bullet B_3O_4$ can occur from only structures **16** and **18**; structure **18** may lose $^\bullet B_3O_4$ by ring cleavage at a and b. The coincident ionic product is $[B_3O_4]^+$ (**2**). B_2O_3 may be lost from structure **17** by simple bond cleavage and from structure **18** by bond cleavage at the B_2O_3 branch or by an RDA-type reaction. Structure **16** does not form a stable ion upon loss of B_2O_3. Structure **18** can convert to structure **16** by ring opening at b or to structure **17** by ring opening at c.

---

(31) March, J. *Advanced Organic Chemistry*; Wiley: New York, 1985, pp 18.

(32) Armstrong, D. R.; Perkins, P. G. *J. Chem. Soc. A* **1967**, 790–792. Dewar, M. J. S.; McKee, M. L. *J. Am. Chem. Soc.* **1977**, *99*, 5231–5241. Haddon, R. C. *Pure Appl. Chem.* **1982**, *54*, 1129–1142. Jug, K. *J. Org. Chem.* **1983**, *48*, 1344–1348.

(33) Barton, L.; Brinza, D.; Frease, R. A.; Longcor, F. L. *J. Inorg. Nucl. Chem.* **1977**, *39*, 1845–1847.

(34) Lehmann, W. J.; Wilson, C. O., Jr. *J. Inorg. Nucl. Chem.* **1961**, *21*, 25–32.

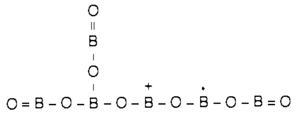
16 $O=B-O-\overset{\overset{O=B-O}{|}}{B}-O-\overset{+}{B}-O-\overset{\bullet}{B}-O-B=O$

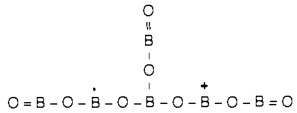
17 $O=B-O-\overset{\bullet}{B}-O-\overset{\overset{O=B-O}{|}}{B}-O-\overset{+}{B}-O-B=O$

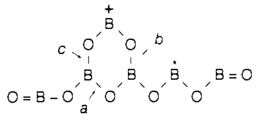
18

The radical ions of series V may achieve a degree of stability through structures that enable electron sharing and resonance analogous to structures **1**–**3**. The canonical forms of $[B_4O_5]^{\bullet+}$ (**12**–**14** and their mirror image forms) demonstrate potentially extensive charge delocalization throughout the central O-B-O-B-O "core" of the ion. Likewise, the higher order series V ion, $[B_6O_8]^{\bullet+}$, may exhibit extensive charge delocalization in structure **16**. On the other hand, another $[B_6O_8]^{\bullet+}$ isomer, structure **17**, would exhibit a more limited charge delocalization because of the centrally located –O—B=O branch.

In conclusion, series V ions show a strong tendency to dissociate by the loss of a series II ion. The numerous resonance forms of acyclic series V ions enhance stability through extensive delocalization of the charge. Some delocalization of the unpaired electron may contribute to the stability of series V ions.

(3) CA Mass Spectra of Series VI Ions. Series VI is composed of the quasi-molecular ion, $[B_2O_3]^{\bullet+}$, and its multimers. The structure of $[B_2O_3]^{\bullet+}$ (**19**) is proposed to be analogous to that for the neutral species (Figure 1b). The losses of O, $^{\bullet}BO$, and $^{\bullet}BO_2$ in the CA mass spectrum of $[B_2O_3]^{\bullet+}$ are consistent with this structure.

$${\bullet}O-\overset{+}{B}-O-B=O$$

19

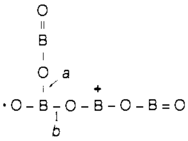
20 $\bullet O-\underset{\underset{b}{|}}{\overset{\overset{O=B-O\ a}{|}}{B}}-O-\overset{+}{B}-O-B=O$

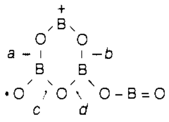
21

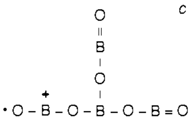
22 $\bullet O-\overset{+}{B}-O-\overset{\overset{O=B-O}{|}}{B}-O-B=O$

The remaining series VI ions show a strong tendency to form a series II ion; loss of $^{\bullet}BO_2$ dominates their CA spectra. Because they exhibit an extensive array of isomeric structures, only $[B_4O_6]^{\bullet+}$ will be discussed in detail. Three isomeric structures of $[B_4O_6]^{\bullet+}$ (**20**–**22**) are shown. Structure **21** can convert to structure **20** or **22** by ring opening at b or a. The dominant loss of BO_2 may occur from all three structures; structure **20** may lose $^{\bullet}BO_2$ by bond breaking at a, structure **22** may lose $^{\bullet}BO_2$ by the breaking of any B–O bond on the tertiary boron atom, and structure **21** may lose $^{\bullet}BO_2$ by ring cleavage at a and b. In all cases the stable $[B_3O_4]^+$ ion (**2**) is formed. Loss of B_2O_3 is possible only from structures **20** and **21**. Structure **20** loses B_2O_3 by bond breaking at b, and structure **21** loses B_2O_3 by an RDA-type reaction with cleavage at b and c. In both cases the ionic product is structure **19**.

The higher order ions of series VI show a strong tendency to form a series II ion upon dissociation; losses of $^{\bullet}BO_2$, $^{\bullet}B_3O_5$, and $^{\bullet}B_5O_8$ are observed. The loss of $^{\bullet}BO_2$ is significantly more probable than the loss of a B_2O_3 molecule, in keeping with the trend of most boron oxide ions to dissociate with the attending formation of a stable series II ion.

(4) CA Mass Spectra of Series I, III, and IV Ions. The ions of these three series appear at significantly lower abundances than those of the three series considered in detail above. Consequently, the CA mass spectra of the higher order members of these series show poor signal to noise ratios. The limited number of spectra available make it difficult to establish dissociation trends within each series.

Series I and IV ions will not be discussed in detail. The CA spectrum of $[B_5O_8]^+$ (series IV) shows artifact peaks originating from metastable processes occurring prior to the magnetic sector. Diagnostically important areas of the spectrum are obscured, and therefore no conclusions can be drawn about series IV. The CA spectrum of $[B_5O_6]^+$ (series I) shows the dissociative loss of B_2O_2 with the formation of $[B_3O_4]^+$ (series II). This is in keeping with the overall trend of boron oxide ions to dissociate by the formation of a stable series II ion. However, the number of CA spectra for series I are insufficient to establish a trend or postulate structures.

Series III ions warrant comment because they exhibit dissociation pathways that suggest the presence of boron–boron bonds. The strongest evidence for this lies in the CA spectrum of $[B_4O_4]^{\bullet+}$. $[B_4O_4]^{\bullet+}$ deviates from the general trend of boron oxide dissociation in that it does not dissociate to yield a series II ion. The ionic dissociation products of $[B_4O_4]^{\bullet+}$ are $[B_2O_2]^{\bullet+}$ (loss of a B_2O_2 molecule) and $[B_3O_3]^+$ (loss of $^{\bullet}BO$). These products are consistent only with a structure containing a B–B bond (**23**). It should be emphasized that structure **23** is speculative; there are no other series of boron oxide ions containing B–B bonds from which to establish likely dissociation mechanisms and to identify stable product ions and product neutrals. In addition, structure **23** must be formed by reactions of fragments within the boron trioxide melt or by the currently debated process of ion–molecule reactions in the high-pressure selvedge region very close to the surface of the sample.[35]

$$O=B-O-\dot{B}-B=\overset{+}{O}-B=O$$

23

Conclusions

Many of the boron oxide ions reported here are analogous to previously reported high molecular weight boron sulfides.[36,37] There are significant differences in both the condensed-phase structures of B_2O_3 and B_2S_3 and experimental methods used to observe their gas-phase oligomers. The structure of crystalline B_2S_3 has been shown to consist of 6-membered B_3S_3 rings and 4-membered B_2S_2 rings joined through sulfur atoms to form $B_{16}S_{16}$ rings.[38] The B–S system was studied by electron ionization of gas-phase species produced by heating crystalline B_2S_3. In contrast to this, the B–O system was studied by high-energy particle bombardment of solid and molten vitreous B_2O_3. These differences notwithstanding, the most abundant boron sulfide ions observed were analogous to the series II and series VI boron oxide ions.

It is difficult to compare the boron–oxygen and boron–sulfur systems because no structures were proposed for boron sulfide ions; the work was completed before the introduction of collision-induced dissociation as a structural probe. Nevertheless, several differences should be noted. There are no series III or higher order series V and series I analogues in the boron sulfide systems ($[B_2S_2]^{\bullet+}$ and $[B_3S_3]^+$ were reported). The reason for this is not clear. There is, however, an adequate explanation for the existence of sulfur-rich boron sulfide ions ($[BS_3]^+$, $[B_2S_4]^{\bullet+}$, $[B_4S_7]^{\bullet+}$, $[B_6S_{10}]^{\bullet+}$, etc.) and the absence of oxygen-rich counterparts in the boron–oxygen system. That is that the boron sulfide species probably contain the S–S bond; the absence of boron oxide analogues owes to the instability of the peroxide bond.[37] In any event, a productive comparison of gas-phase boron sulfide ions and boron oxide ions

---

(35) Pachuta, S. J.; Cooks, R. G. *Chem. Rev.* **1987**, *87*, 647–669.

(36) Green, F. T.; Giles, P. W. *J. Am. Chem. Soc.* **1962**, *84*, 3598–3599. Greene, F. T.; Gilles, P. W. *J. Am. Chem. Soc.* **1964**, *86*, 3964–3969. Chen, H.; Gilles, P. W. *J. Am. Chem. Soc.* **1970**, *92*, 2309–2312. Chen, H.; Gilles, P. W. *J. Phys. Chem.* **1972**, *76*, 2035–2038.

(37) Edwards, J. G.; Gilles, P. W. *Mass Spectrometry In Inorganic Chemistry*; Gould, R. F., Ed.; American Chemical Society: Washington, DC, 1968; pp 211–230.

(38) Wells, A. F. *Structural Inorganic Chemistry*; Clarendon: Oxford, 1984; pp 1045–1046.

will have to await more detailed work on boron sulfide structures.

In conclusion, gas-phase boron oxide ions are formed by particle-induced desorption from condensed-phase (vitreous) boron trioxide by random B–O bond breaking at any site along the $(B_2O_3)_n$ network. The relative abundances of boron oxide ions are directly related to the relative stabilities of the desorbed ions. Relatively less stable boron oxide ions are more likely to undergo dissociation during the ca. 23×10^{-6} s flight time from ion source to detector (ZAB-2F mass spectrometer, ion of m/z 100, 8-kV accelerating voltage[39]). The relative stability of a desorbed boron oxide ion is also related to the ability of its structure to satisfy the +3 oxidation state of boron; there is no indication that boron exists in other than the +3 oxidation state in the boron oxide cations reported here. Accordingly, boron oxide structures incorporate integral BO_3 units and terminal –B=O units. Stability is enhanced by resonance forms and electron sharing that achieve delocalization of the charge on the cation.

Finally, it is important to note the structural differences between the new boron oxide cations reported here and the large (and growing) body of known, condensed-phase, borate anions.[40] Borate anions typically contain both three-coordinated BO_3 units and four-coordinated (tetrahedral) BO_4^- units in association with metal cations. The insular boron oxide cations, however, are unable to accommodate the negative charge and contain only three-coordinated BO_3 units and two-coordinated –B=O units.

Acknowledgment. The author expresses his gratitude to E.B.D.

Registry No. B_2O_3, 1303-86-2.

---

(39) Holmes, J. L. *Org. Mass Spectrom.* **1985**, *20*, 169–183.

(40) Heller, G. In *Topics In Current Chemistry: Structural Chemistry of Boron and Silicon*; Boschke, F. L., Ed.; Springer-Verlag: Heidelberg, 1986; pp 39–98.

An NMR Method for Distinguishing Classical from Nonclassical Structures in Transition-Metal Polyhydrides

Douglas G. Hamilton and Robert H. Crabtree*

Contribution from the Department of Chemistry, Yale University, New Haven, Connecticut 06511. Received June 15, 1987

Abstract: A T_1 method is described for distinguishing classical hydrides with terminal M–H bonds from nonclassical hydrides with H–H as well as M–H bonds. The method can still be used even where the hydrides are fluxional as is the case for transition-metal polyhydrides. The temperature dependence of the T_1 shows a minimum for several cases studied. This allows the H–H distance in the H_2 ligand to be estimated and the structural type determined. $ReH_7(PPh_3)_2$ is shown to be nonclassical with the probable structure $Re(H_2)H_5(PPh_3)_2$. $[ReH_8PPh_3]^-$ is shown to be classical and $[ReH_9]^{2-}$ seems to be classical, however. Other hydrides shown to be nonclassical are $Re(H_2)H_5(dpe)$, $FeH_2(H_2)L_3$, $RuH_2(H_2)L_3$, and $[Os(H_2)H_3(PPh_3)_3]^+$; the Re examples are the first d^2 and the Os example the first d^4 dihydrogen complex. Complexes shown to be classical are the following: $IrH_5(PCy_3)_2$, $ReH_5(PPh_3)_3$, $OsH_4(P\{p\text{-tolyl}\}_3)_3$ $MoH_4(PMePh_2)_4$, and, more surprisingly, $[WH_5(PMePh_2)_4]^+$, $H_2Fe(CO)_4$, $[IrH_2(CO)_2(PPh_3)_2]^+$, and $WH_6(PMe_2Ph)_3$. Typical distance estimates (r_{eff}) obtained are the following: $[IrH(H_2)(bq)(PPh_3)_2]^+$, 1.04$C$ Å; $ReH_5(H_2)(PPh_3)_2$, 1.20C Å; $ReH_5(H_2)(dpe)$, 1.25C Å; $MoH_4(PMePh_2)_4$, 1.72C Å, where C is a calibration constant (as yet undetermined but ~0.9). The ordering of the r_{eff} values observed seems to parallel the relative lability order of the complexes studied, the more labile species being associated with shorter r_{eff} values.

We describe in detail a T_1 method for determining whether a given transition-metal hydride has a classical structure, with all terminal M–H bonds (**1**) or a nonclassical structure, with one or more H–H bonds. An example of such a structure is dihydrogen complex **2**. In 1984 Kubas et al.[1] first showed that structures of type **2** could exist. Since that time several other examples have been discovered both by ourselves[2] and by others.[3] Kubas et al.[1] used neutron diffraction, IR, and the $^1J(H,D)$ in the ^1H NMR spectrum of the HD complex to characterize their complex. Morris[3a,f] has used IR, NMR, and X-ray methods. Neutron diffraction is more reliable than X-ray but requires large crystals. IR data can be unreliable because the $\nu(MH_2)$ absorption is often too weak to be seen. $^1J(H,D)$ can only be observed if fluxionality does not interfere. It is precisely for the most interesting group of candidate structures, metal polyhydrides,[4] that rapid fluxionality is most common.

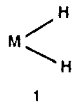

1

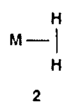

2

---

(1) (a) Kubas, G. J.; Ryan, R. R.; Swanson, B. I.; Vergamini, P. J.; Wasserman, J. J. *J. Am. Chem. Soc.* **1984**, *106*, 451–2. (b) Wasserman, J. J.; Kubas, G. J.; Ryan, R. R. *J. Am. Chem. Soc.* **1986**, *108*, 2294–2301. (c) Kubas, G. J.; Unkefer, C. J.; Swanson, B. I.; Fukushima, E. *J. Am. Chem. Soc.* **1986**, *108*, 7000–9.

(2) (a) Crabtree, R. H.; Lavin, M. *Chem. Commun.* **1985**, 794–5. (b) Crabtree, R. H.; Lavin, M. *Chem. Commun.* **1985**, 1661–2. (c) Crabtree, R. H.; Lavin, M.; Bonneviot, L. *J. Am. Chem. Soc.* **1986**, *108*, 4032–37. (d) Crabtree, R. H.; Hamilton, D. H. *J. Am. Chem. Soc.* **1986**, *108*, 3124.

(3) (a) Morris, R. H.; Sawyer, J. F.; Shiralian, M.; Zubkowski, J. D. *J. Am. Chem. Soc.* **1985**, *107*, 5581–2. (b) Upmacis, R. R.; Gadd, G. E.; Poliakoff, M.; Simpson, M. B.; Turner, J. J.; Wyman, R.; Simpson, A. F. *Chem. Commun.* **1985**, 27–30. (c) Church, S. P.; Grevels, F.-W.; Herman, H.; Schaffner, K. *Chem. Commun.* **1985**, 30–2. (d) Conroy-Lewis, F. M.; Simpson, S. J. *Chem. Commun.* **1986**, 506. (e) Conroy-Lewis, F. M.; Simpson, S. J. *Chem. Commun.*, **1987**, 1675–6 and personal communication. (f) Bautista, M.; Earl, K. A.; Morris, R. H.; Sella, A. *J. Am. Chem. Soc.* **1987**, *109*, 3780. (g) Bianchini, C.; Mealli, C.; Peruzzini, M.; Zanolini, F. *J. Am. Chem. Soc.* **1987**, *109*, 5548–9. (h) Bautista, M. T.; Earl, K. A.; Maltby, P. A.; Morris, R. H.; Sella, A. *J. Am. Chem. Soc.*, submitted and personal communication, 1988. (i) Arliguie, T.; Chaudret, B.; Devillers, J.; Poilblanc, R. *C. R. Acad. Sci. (Paris) Ser. II* **1987**, *305*, 1523. (j) Heinekey, D. M.; Payne, N. G.; Schulte, G. K. *J. Am. Chem. Soc.* **1988**, *110*, 2303–5.

(4) Hlatky, G. G.; Crabtree, R. H. *Coord. Chem. Rev.* **1985**, *85*, 1–48.

0002-7863/88/1510-4126$01.50/0